# PRELIMINARY DESIGN OF A MULTI- STAGE AXIAL COMPRESSOR

**Prof. Dr.Munther I. Al-Druby**
**Mech. Eng. Dept.**
**College of Engineering**
**University of Baghdad**
**Baghdad - Iraq**

**Prof. Dr. Ihsan Y. Hussain**
**Mech. Eng. Dept.**
**College of Engineering**
**University of Baghdad**
**Baghdad - Iraq**

**Ruqeaa Ismail M. Al-Rubyee**
**Ministry of Science and Technology**
**Space & Aeronautics Research Center**
**Turbomachine Dept.**
**Baghdad - Iraq**

**ABSTRACT**

A numerical calculations algorithm has been developed in the present work for a thermodynamics and aerodynamic design of an axial flow compressor. The design calculations were based on thermodynamics, gas dynamic, fluid mechanics, aerodynamic and empirical relations. A two- dimensional compressible flow is assumed with constant axial and rotor blade velocities. A free –vortex swirl distributions was used in the design. These calculations include; power of the compressor, thermodynamic properties of the working fluid, stage efficiency, number of rotor and stator blades, tip and hub diameters, blade dimensions (chord, length and space) for both rotor and stator, velocity triangles before and after the rotor, Mach number, solidity, degree of reaction, flow and blade angles (blade twist) and lift and drag coefficients along the blade and lift. A repeated stage calculation is made to calculate the above parameters along compressor stages. The twist of the blades can be calculated along the blade length at any required number of sections selected by the designers to obtain smooth blade twist profile. The developed algorithm was tested on a compressor cascade series type NACA 65(12)10 with circular camber angle of (30°). The results show that; the lift coefficient decreases as mean flow angle increases, the drag coefficient increases along blade length at a mean flow angle of (15°), the relative Mach number increases along blade length as mean flow angle increases, the ratio of total drag coefficient to lift coefficient increases when the mean flow angle increases, the drag coefficient decreases along blade length as the solidity increases, the cascade efficiency increases as the mean flow angle increase to (45°).

**الخلاصة:**

تم في هذا البحث تطوير خوارزمية حسابات عددية للتصميم الثرموديناميكي والايروديناميكي لضاغطة محورية. تم في هذه الحسابات التصميمية اعتماد معادلات الثرموديناميك, ديناميك الغازات, ديناميك الموائع, الايروديناميك و بعض العلاقات التجريبية بالاعتماد على الفرضيات التالية: اعتبار الجريان ثنائي البعد وانضغاطي, ثبوت السرعة المحورية وسرعة الريشة الدوارة والتوزيع الدوامي الحر لالتواء الريش. تم في هذه الخوارزمية ايجاد اهم الخواص واكثرها فاعلية في حسابات تصميم الضاغطة.

تم ايجاد قدرة الضاغطة وخواص المائع الحرارية للريش الدوارة والثابتة, كفاءة المرحلة الواحدة, عدد الريش الدوارة والثابتة, الاقطار عند قمة وقاعدة الريشة بثبوت قطر وسط الريشة, ابعاد الريشة الدوارة والثابتة (طول, عرض و وتر), مثلثات السرع قبل

وبعد الريشة الدوارة, رقم ماخ النسبي, النسبة الفراغية, درجة رد الفعل, زوايا الجريان وزوايا الريش الدوارة والثابتة ( التواء الريش) ومعامل الرفع على طول الريشة. تم اجراء حسابات لتحديد التواء الريش عن طريق اختيار عدد من النقاط على طول الريشة(حسب رأي المصمم) والحصول على درجة التواء مقبولة. تم اعتماد أسلوب حسابات المرحلة المتكررة لتسهيل الانتقال من صف إلى آخر أو خلال مراحل الضاغطة. تم إجراء اختبار خوارزمية الحسابات العددية على متعاقبة من سلسلة الضواغط نوع NACA65(12)10ذات معدل تحدب دائري وزاوية تحدب (30) درجة. أظهرت النتائج إن معامل الرفع يقل بزيادة متوسط زاوية الجريان, يزداد معامل الكبح عند اقل متوسط زاوية جريان, ازدياد رقم ماخ عند زيادة متوسط زاوية الجريان, زيادة نسبة معامل الكبح الكلي الى معامل الرفع بزيادة متوسط زاوية الجريان, يقل معامل الكبح على طول الريشة عند زيادة النسبة الفراغية, تزداد كفاءة المتعاقبة عند زيادة متوسط زاوية الجريان وصولا الى زاوية مقدارها (45) درجة بعده تبدأ بالنقصان تدريجيا.

**KEYWORDS**
**Axial Compressor, Multi-Stage, Preliminary design**

## INTRODUCTION

Axial compressor is one of the most common compressor types in use today. It finds its major application in large gas turbine engine like those of power today's jet aircraft, it derive its name from the fact that the air being compressed has very little motion in the radial direction, in contrast, the radial motion of the air in centrifugal compressor is much longer than the axial motion **(Yahya 1983)**. In general, the axial machines have much greater mass flow but much less pressure ratio per stage because of the boundary layer behavior, fundamentally, the axial compressor is limited by boundary layer behavior in adverse (positive) pressures gradients, each blade passage of compressor may be thought of as a diffuser, so that the boundary layer on all its wall are subject to a pressure increase unless this pressure gradient is kept under control, separation or stall will occur **(Peterson 1970)**. The compressor is made up of two major assemblies. The rotor with its blades and the casing with its stationary blades (stator) and this make one stage, the rotor increase the angular velocity of the fluid resulting increase in total temperature, total pressure and static pressure. The following stator decrease the angular velocity of the fluid, resulting in an increase in the static pressure and sets the flow up for the following rotor **(Mattingly 1996)**.

The axial compressor may be designed with constant tip diameter or with constant mean diameter or with constant hub diameter or with all varying; however the mean blade radius does not usually change very much. The blade length varies in order to accommodate the variation in air density so that the axial velocity component will be approximately uniform. **(Vincent 1950)**

## THEORETICAL FORMULATION

A theoretical and empirical formulation of design calculations for a multi -stage axial flow compressor is developed. The formulation will be based on a thermodynamic, gas dynamic, fluid mechanics and aerodynamic relations. Besides; an empirical correlations and values for some design parameters will also be used. The design calculations include, in general, the number of stages, rotor and stator blades data (numbers, width, pitch, height and twist angles), annular area distribution along the compressor, the thermodynamic state along the compressor section and along the blade height at each section, lift and drag for both stator and rotor blades along the compressor, the degree of reaction along the blade height for each stage, the power required to drive the compressor, Mach numbers and the velocity diagram at the rotor inlet and outlet along the blade height.**(Al- Rubyee 2006)**

### Power of the Compressor:

From the general momentum equation (Peterson 1970);

$$\Sigma F = \frac{d}{dt}\int_{cv} \rho V_u dv + \int_{cs} \rho V_u (V_u \cdot n) dA \quad (1)$$

It can be shown that the

$$P_{sh} = \dot{m} U (r_2 V_{2u} - r_1 V_{1u}) \quad (2)$$

Where $U = \omega * r$ & for the axial machines, ($r_2 = r_1$ )

And, the power required to drive the compressor is calculated as;

$$\textbf{Power} = P_{sh} / \eta_c \quad (3)$$

**Compressor Efficiencies:**

By using the definition of the compressor efficiency: [Mattingly 1996]

$$\eta_c = \frac{h_{nss} - h_1}{h_n - h_1} = \frac{T_{nss} - T_1}{T_n - T_1} \quad (4)$$

$$\eta_c = \frac{(P_n/P_1)^{\frac{\gamma-1}{\gamma}} - 1}{(P_n/P_1)^{\frac{\gamma-1}{\gamma \eta s}} - 1} \quad (5)$$

Using the (h-s) diagram, the stage efficiency can be obtained as;

$$\eta_s = \frac{(T_{3ss}/T_1) - 1}{\frac{T_3 - T_1}{T_1}} \quad (6)$$

**Radial Equilibrium**:

For long blades, the variations of blade speed, static pressure and the axial velocity are considerable and the three – dimensionality must be taken into account. The basic assumption of the radial equilibrium type of design is that the radial velocity component is zero at entry and exit from a blade row. The basic equation of motion is (Peterson 1970);

$$\frac{1}{\rho}\frac{\partial P_o}{\partial r} = \frac{V_u^2}{r} + V_u \frac{\partial V_u}{\partial r} + V_x \frac{\partial V_x}{\partial r} \quad (7)$$

Using the exponential swirl distribution type of design, where the swirl velocity ($V_u$) at the inlet and exit to the rotor has the following general variation with radius (Dixon 1975);

$$V_{1u} = a r^n - \frac{b}{r} \quad \& \quad V_{2u} = a r^n + \frac{b}{r} \quad (8)$$

Where (a) and (b) are constants and the index (n) have any value, but in exponential swirl distribution the index is taken to be equal to zero (n=0**)**.

Note that, the axial velocity at the rotor inlet and exit is the same along the mean line, but at other section the axial velocity will be calculated at inlet and outlet as follows:

Differentiating **eq.(8)** and substitute the results in **eq.(7)** to get the variation of axial velocity as;

$$V_{x1}^2 = k_1 - 2a^2\left[\ln(r) + \frac{b}{ar}\right] \quad \& \quad V_{x2}^2 = k_2 - 2a^2\left[\ln(r) - \frac{b}{ar}\right] \quad (9)$$

$(k_1)$ and $(k_2)$ can be evaluated at constant axial velocity in the mean line section and taking the same for all blade section.

**Thermodynamic Calculations:**

The thermodynamic properties at stage inlet (rotor) are calculated from equations below (Mattingly 1996)**;**

$$P_1 = P_{o1} * \left(\frac{T_1}{T_{o1}}\right)^{\gamma/\gamma-1} \quad (10)$$

$$h_1 = C_P * T_1 \quad (11)$$

The isentropic stagnation and static temperature can be found from:

$$T_{o3ss} = T_{o1} * \left(\frac{P_{o3}}{P_{o1}}\right)^{\frac{\gamma-1}{\gamma}} \quad \& \quad T_{3ss} = T_{03ss} - \frac{V_3^{\,2}}{2C_P} \tag{12}$$

Also, the static isentropic enthalpy can be obtained as;

$$h_{3ss} = C_P \ {}^{*}T_{3ss} \tag{13}$$

Now, $$\Delta h_{is} = h_{3ss} - h_1 \quad \& \quad \Delta h_{rotor} = R_C * \Delta h_{is} \tag{14}$$

Where ($R_C$) is the degree of reaction.

Thus $$h_{2is} = h_1 + \Delta h_{rotor} \tag{15}$$

$$T_{2is} = h_{2is} / C_P \tag{16}$$

Now, the pressure, temperature, density and enthalpy at rotor exit can be calculated as;

$$P_2 = P_1 * \left(\frac{T_{2is}}{T_1}\right)^{\frac{\gamma}{\gamma-1}} \quad \& \quad T_2 = \frac{h_2}{C_P} \tag{17}$$

$$\rho_2 = \frac{P_2}{R * T_2} \quad \& \quad h_2 = h_1 + 0.5 * \left(w_{1m}^{\,2} - w_{2m}^{\,2}\right) \tag{18}$$

Note that, the terms ($w_{1m}$ and $w_{2m}$) in **eq.(18)** were calculated from velocity triangle at mean section, as will be explained later; the stagnation temperature loss at mean section can be calculated as;

$$\frac{\Delta T_o}{T_{o1}} = \left(\frac{U_m^{\,2}}{C_P * T_{o1}} * \frac{V_{xm}}{U_m} * \tan\beta_{1m}\right) - \left(\frac{V_{xm2}}{V_{xm1}} * \tan\beta_{2m}\right) \tag{19}$$

**Degree of Reaction:**

A useful term for turbomachine designers is the degree of reaction which is defined as the ratio of the static enthalpy increase across the rotor to the increase in static enthalpy for the stage.

$$R_c = \frac{\Delta h_{rotor}}{\Delta h_{stage}} = \frac{h_2 - h_1}{h_3 - h_1} \tag{20}$$

Or, using the notation for the axial flow stage as shown in **Fig.(1)** (Yahya 1983);

$$R_c = \frac{w_1^{\,2} - w_2^{\,2}}{2U(V_{2u} - V_{1u})} \tag{21}$$

**Aerodynamic Calculations:**

To evaluate the lift and drag forces, lift and drag coefficients must be calculated as shown below:

The mean relative velocity for rotor can be obtained as (Bathie 1995);

$$w_m = \frac{(w_1 + w_2)}{2} \ \& \ w_{um} = \frac{(w_{1u} + w_{2u})}{2} \tag{22}$$

And mean angle **($\beta_m$)** for rotor can be obtained from:

$$\beta_m = \tan^{-1}\left(\frac{w_{um}}{V_{xm}}\right) \tag{23}$$

**Cascade Test:**

From typical cascade test (Peterson 1970) for blade type NACA 65 (12) 10 at solidity equal one (c/s =1) and by using curve -fitting program, the equation relates the cascade angles to the stagger angle were obtained from:

$$\beta_{ii} = -25.3 + 0.228 * \beta_i + 0.929 * \lambda \quad (24)$$

This equation can be applied at ($\lambda$) values between (10° - 50°) and ($\beta_i$) between (30°-70°) to calculate the angle at cascade exit ($\beta_{ii}$) and these will be taken as the same for all stages.

For rotor: $\beta_i = \beta_1$ , $\beta_{ii} = \beta_2$

For stator: $\beta_i = \alpha_2$ , $\beta_{ii} = \alpha_3$

$$C_L = 2\frac{s}{c}\cos\beta_m\left(\tan\beta_i - \tan\beta_{ii}\right) - \frac{\Delta P_o}{\rho w_m^2/2} * \frac{s}{c}\sin\beta_m \quad (25)$$

$$C_D = \frac{\Delta P_o}{\rho w_m^2/2} * \frac{s}{c}\cos\beta_m \quad (26)$$

The total effective drag coefficients for the cascade (using the notations of the present work for length) may be written as;

$$C'_D = (C_D)_{cascade} + 0.02(s/L) + 0.018C_L^2 \quad (27)$$

**Pressure Rise Limitations:**

The limiting pressure coefficient can be expressed for a simple case in terms of blade angles, in which the blades may be either rotor or stator blades, since the axial velocity is constant at inlet and outlet to cascade, where many designers limit the static pressure rise in a given blade row to $C_P < 0.6$ (Peterson 1970), therefore :

$$C_P = 1 - \frac{\cos^2\beta_i}{\cos^2\beta_{ii}} \quad (28)$$

**Compressibility Effects:**

Compressibility limits the relative velocity at the inlet to any blade row, and this limitation is especially important for the first stage of the axial flow compressor. The relative Mach number at rotor entrance usually lies in the range of $0.6 < M_{1rel} < 0.85$ and it can be calculated as (Peterson 1970);

$$M_{1rel} = \frac{w_1}{\sqrt{(k * R * T_1)}} \quad (29)$$

**Annular Area Distribution**

**Constant Mean Diameter( see Fig. 2-a):**

By assuming the design radius of the compressor stage is at the mean line, this leads to:

$$D_m = D_{m1} = D_{m2} = D_{m\,n}$$

From equations below the area, mean diameter and length at stage inlet can be computed as;

$$A_1 = \frac{\dot{m}}{\rho_1 * V_{xm}} \quad \& \quad L_1 = \frac{A_1}{\pi * D_m}, \quad r_m = D_m / 2 \quad (30)$$

Thus, the tip and hub (root) diameter is obtained from:

$$D_{t1} = D_m + L_1 \quad \& \quad D_{r1} = D_m - L_1$$

Similarly, in the same way can be found all dimensions at rotor exit or at stage exit.

**Constant Root Diameter ( see Fig. 2-b):**

The root diameter can be defined as;

$$D_r = D_{m1} - L_1$$

From assumption of constant root diameter: $D_r = D_{r1} = D_{r2} = D_{r3} = D_{r\,n}$

Now, the tip diameter at inlet to the stage is:

$$D_{t1} = D_r + 2L_1 \quad (31)$$

Again, by using the continuity equation the tip diameter at rotor exit can be calculated as;

$$\dot{m} = \rho_{m2} V_{xm} * \frac{\pi}{4}(D_{t2}^2 - D_r^2) \quad \& \quad D_{t2} = \sqrt{\frac{4\dot{m}}{\rho_{m2} V_{xm} * \pi} + D_r^2} \quad (32)$$

So, the length and mean diameter at rotor exit can be found from:

$$L_2 = \frac{D_{t2} - D_r}{2} \quad \& \quad D_{m2} = D_r + L_2 \quad (33)$$

**Constant Tip Diameter ( see Fig. 2-c):**

The tip diameter can be defined as;

$$D_t = D_{m1} + L_1$$

Also, from assumption of constant tip diameter: $D_t = D_{t1} = D_{t2} = D_{t3} = D_{t\,n}$

Now, at inlet to the stage: $D_{r1} = D_t - 2L_1$

Again, by using the continuity equation, the tip diameter at rotor exit is;

$$\dot{m} = \rho_{m2} V_{xm} * \frac{\pi}{4}(D_t^2 - D_{r2}^2) \quad \& \quad D_{r2} = \sqrt{D_t^2 - \frac{4\dot{m}}{\rho_{m2} V_{xm} * \pi}} \quad (34)$$

So, the length and mean diameter at rotor exit can be found from:

$$L_2 = \frac{D_t - D_{r2}}{2} \quad \& \quad D_{m2} = D_t - L_2 \quad (35)$$

**Number of Blades:**

To specify the number of blades for both rotor and stator, suitable limit for aspect ratio and solidity must be assumed. The aspect ratio is defined as;

$$AR = \frac{L}{c} \quad (36)$$

The space can be obtained from equation of solidity ($\sigma$.) as;

$$\sigma = \frac{c}{s} \quad (37)$$

$\therefore$ The number of rotor blades can be evaluated as;

$$n = \frac{(2 * \pi * r_m)}{s} \quad (38)$$

The number of blades must be a whole number, if not an interpolation for the blades number must be and recalculate in the reverse order then yields a new space, chord and aspect ratio as (Cohen 1972);

$$s = \frac{(2 * \pi * r_m)}{n} \quad , \quad c = \sigma * s \quad \& \quad AR = \frac{L}{c} \quad (39)$$

The calculations of chord, space and number of blades for the stator is made in a similar procedure as mentioned above, but the solidity of the stator blades is usually less than that for the rotor blades (Vincent 1950).

**Blade Twist**

**Blade Angle**: The blade inlet angle will be known when chosen incidence angle at the design point, equal to zero, but the blade outlet angle can not be determined until the deviation angle ($\delta$**)** has been determined (Cohen 1972) by using the Howells relations;

$$\delta = m\theta\sqrt{(s/c)} \quad , \quad \text{where : } m = 0.23(2\frac{a}{c})^2 + 0.1(\frac{\beta_2}{50}) \quad (40)$$

For circular arc camber (2a/c) =1(Cohen 1972), and (a) is the distance of point of maximum camber from the leading edge of the blade.

In terms of rotor blades;

$$\theta = \beta'_1 - \beta'_2 \quad \& \quad \delta = \beta_2 - \beta'_2 \tag{40a}$$

From **eq.( 40a & 40)** and using zero incidences (i.e. $\beta_1 = \beta'_1$ : $\alpha_1 = \alpha'_1$) can be get:

$$\theta = \frac{\beta_1 - \beta_2}{\left(1 - m\sqrt{s/c}\right)} \tag{41}$$

**Velocity Triangle Calculation at Mean Section**

It is important to be able to calculate the change in tangential velocity across the rotor (Dixon 1975). This is best accomplished by drawing velocity diagrams for a normal compressor stage as shown in **Fig.(1)**.

The velocity diagrams at the mean section may calculate as follows:

The inlet absolute velocity from:

$$V_{1um} = V_{xm} * \tan(\alpha_{1m}) \quad \& \quad V_{1m} = \sqrt{\left(V_{xm}^{\ 2} + V_{1um}^{\ 2}\right)}$$

And the inlet relative velocity as; (42)

$$w_{1um} = U_m - V_{1um} \quad \& \quad w_{1m} = \sqrt{\left(V_{xm}^{\ 2} + w_{1um}^{\ 2}\right)}$$

Where the $V_{1um}$ & $w_{1um}$ is the component velocity of $V_{1m}$ & $w_{1m}$ and by applying the set of equations below, the outlet absolute velocity can be calculated from:

$$w_{2um} = \sqrt{\left(w_{2m}^{\ 2} - V_{xm}^{\ 2}\right)}, \quad V_{2um} = U_m - w_{2um} \quad \& \quad V_{2m} = \sqrt{\left(V_{xm}^{\ 2} + V_{2um}^{\ 2}\right)} \tag{43}$$

Now, the flow angles related to the relative inlet and outlet velocity were calculated as:

$$\beta_{1m} = \tan^{-1}\left(w_{1um} / V_{xm}\right) \quad \& \quad \beta_{2m} = \tan^{-1}\left(w_{2um} / V_{xm}\right) \tag{44}$$

Also, the outlet flow angles related to the outlet absolute velocity can be calculated as;

$$\alpha_{2m} = \tan^{-1}\left(V_{2um} / V_{xm}\right) \tag{45}$$

The constants (a) & (b) is obtained by evaluating the **eq.(8)** at the mean radius as;

$$a_1 = \frac{V_{1um} + V_{2um}}{2} \quad \& \quad b_1 = \frac{r_m\left(V_{1um} - V_{2um}\right)}{2}$$

Also, the constants ($k_1$)& ($k_2$) can be calculated from **eq.(9)** at constant axial velocity in the mean section ;

$$k_1 = V_{xm}^{\ 2} + 2a^2\left(\ln r_m\right) + \frac{b}{ar_m} \quad \& \quad k_2 = V_{xm}^{\ 2} + 2a^2\left(\ln r_m\right) - \frac{b}{ar_m}$$

**RESULTS AND DISCUSSION**

A verification of the proposed theoretical formulation is made here through a comparison between the present work results and the published results of preliminary design of axial flow compressor (Al-Druby and Hussain 1995), the results of calculations for the present work and this case are summarized in **(Tables 2 to 9)** with the given input data listed in **Table (1).**

The length, root and tip diameters are shown in **Table (2)** at inlet, exit from rotor and stage exit at constant mean diameter. The root diameter increases from inlet to exit stage, whereas the tip diameter and length decreases from inlet to exit, these diameters forms the compressor stage geometry, the hub diameter and tip diameter are between (0.306-0.320) and (0.501-0.491), respectively. The number of blades, chord length, and space are shown in **Table (3)**, the calculated aspect ratio for rotor and stator blades is also tabulated. the aspect ratio were calculated after re-calculating the number of blades and space, calculated aspect ratio is less than the assuming value in the given data. The stage exit pressure and temperature, stage efficiency, stagnation temperature rise for one stage, compressor efficiency, pressure and temperature at compressor exit, and the

power required are shown **Table (4)**. The pressure, temperature and density along blade length are shown in **Table (5)**, all thermodynamic properties are increasing from hub to tip radius and the shadow lines represents the mean line data. The lift coefficient result along blade length are shown in **Table (6)** the shadow line represents the mean line data, the lift coefficient increases above the mean line and decreases below the mean line, the lift coefficient is proportional to solidity ratio were calculated. The twist angles at inlet and outlet from rotor and stator, camber angles and relative Mach number along the blade length are shown in **Table (7)**, all the angles increases except the camber angles for rotor which decreases along blade length, the values of relative Mach No. (0.55-0.70) and these value are in the limiting range. The variation of solidities for rotor and stator, degree of reaction along blade length are shown in **Table (8)**, the solidity decreases whereas degree of reaction increases along blade length, the shadow line represents the mean line data and these values is approximately equal to the input data, the solidity in the present work were calculated after re- calculating chord length and space values for the stator are higher than the rotor, thus; the solidity for rotor is less than for the stator along blade length. The results of cascade lift and drag coefficient and effective drag coefficient (total) on the mean line design are shown in **Table (9)**, by using the cascade test curve (Peterson 1970), were chosen the stagger angle of (40°) and inlet cascade angle of (50°) to obtain cascade outlet angle from equ.(24), then applying equ.(28) to find the pressure coefficient ($C_P$) equal to (0.51) and this value is less than the limiting range. the term ($C_D$) and ($C_L$) is for cascade where the term ($C_{Dtotal}$) is for actual compressor blades, by using the value of ($C_{Dtotal}$), the actual stagnation pressure ($\Delta P_O$) for rotor and stator can be obtained to yield the lift and drag forces for actual compressor. The flow angles and the swirl velocity distribution at inlet and exit of the rotor for the present work are shown in **(Figs. 3 and 4)**. There is a significant variation with blade length of the swirl velocity and flow angles near the blade root and very little near the tip, the relative flow turns about (65°) at the hub and only about (39°) at the tip. The large radial variation in the rotor inlet flow angle for one stage requires that its rotor blade have a lot of twist in them. (Mattingly1996). The relative Mach No. along blade length are shown in **Fig.(5)**, the values of the Mach number are between (0.55- 0.7), and these values in the limiting range leads to efficient operation. The advantage of high Mach No. operation is that the mass flow per unit area and the pressure ratio per stage will both be high. Also a parametric case study will be made in different solidities and mean flow angle, the plot of lift and drag coefficients at three solidities (1, 1.33, and 2) along the blade length are shown in **(Figs. 6 and 7)**, the lift coefficient decrease as solidity increases, taking the solidity of one as a reference, the rate of change in lift curve slope for solidity of (1.33) is approximately half that change for solidity of (2), the difference is due to the interference of two opposing effects, the $1^{st}$, is that large blade spacing increase the lift, the $2^{nd}$ , is that close blade spacing mean that the flow angle leaving a blade row exhibits smaller variation a cross the blade passage (Jassam1992), the drag coefficient increases at the tip diameter, then decreases at hub diameter, the drag coefficient increases as solidity decreases, the values of drag coefficient at solidity (1) are between (0.025-0.027) whereas at solidity (2) the values are between (0.037-0.042). A plot of lift and drag coefficients along the blade length at different mean flow angles (15°, 25° ,35° and 45°) are shown in **(Figs. 8 and 9),** where the lift coefficient decreases as mean flow angle increases, till it reaches 45°, the lift coefficient is nearly a straight line, on the other hand, the drag coefficient increases with mean flow angle, up to a value of (45°) then it decreases. The efficiency of compressor cascade with different mean flow angles (15° to 75°) as shown in **Fig.(10)** at varying ratio of ($C_D/C_L$) calculate from the following equation (Dixon 1975);

$$\eta = 1 - \frac{2C_D}{C_L \sin 2\alpha_m} \qquad (46)$$

The maximum efficiency of compressor cascade is obtained when the mean flow angle only a little less than 45° but the curve is rather flat for a wide range in mean flow angle.

## CONCLUDING REMARKS

A suitable design calculations algorithm has been developed for a multi-stage axial flow compressor. The lift coefficient decreases along the blades length from hub to tip. The upper limit of lift coefficient is when the solidity equals one. The lift coefficient decreases as mean flow angle increases, approximately to optimum value at (45°) then the lift coefficient varied little along blade length. The drag coefficients reach higher limits along blade length when the mean flow angle is (15°). The relative Mach No. increases along blade length, but when mean flow angle increases the relative Mach No. decreases.

## REFERENCES

Cohen, H. and Rogers, G. F. C., and Sravanamuttoo, H. I. H., "Gas Turbine Theory", Longman Group Limited, 2nd 1972.

Hill, P. G. and Peterson, C. R. "Mechanics and Thermodynamic of Propulsion", Addison – Wesley Publishing Company, Third Addition, 1970.

Jack D. Mattingly, "Elements of Gas Turbine Propulsion", McGraw- Hill Book, Inc. 1996.

M. I. AL- Durby and I. Y. Hussain "Preliminary Design Calculations for Axial- Flow Turbines and Compressors"; University of Baghdad /Collage of Engineering /Mechanical Department, Technical Report, 1995.

Nayef, T. Jassam, "Parametric Study of Deviation in Axial Flow Compressor", M.Sc., Thesis, Baghdad University, 1992.

Ruqeaa Ismail M. Al- Rubyee, " Preliminary Design of A Multi- Stage Axial Compressor" M.Sc., Thesis, Baghdad University / College of Engineering /Mechanical Dept. , 2006.

S L., Dixon, "Fluid Mechanics, Thermodynamics of Turbomachinery", 2nd Edition, 1975. S M Yahya,., "Turbines, Compressors and Fans", TATA McGraw- Hill, 1983.

S. M Yahya,., "Turbines, Compressors and Fans", TATA McGraw- Hill, 1983.

Vincent, E. T., "The Theory and Design of Gas Turbines and Jet engines", McGraw- Hill Book Company, Inc. 1950.

William W. Bathie, "Fundamentals of Gas Turbines", John Wiley and Sons, Inc., 2nd Edition, 1995.

## NOMENCLATURE

**Latin Symbols**

**Greek Symbols**

| Symbol | Description | Units |
|---|---|---|
| α | Stator Flow Angle | degree |

| | | |
|---|---|---|
| ά | Stator Blade Angle | degree |
| β | Rotor Flow Angle | degree |
| β′ | Rotor Blade Angle | degree |
| γ | Ratio of Specific Heat | ---- |
| δ | Deviation Angle | degree |
| ε | Strain | |
| λ | Stagger Angle | degree |
| ρ | Density | $kg/m^3$ |
| σ | Solidity | ---- |
| θ | Camber Angle | degree |
| Δ | Change per Stage | ---- |
| **ω** | Rotating Speed | r.p.m |
| ∏ | Pressure ratio | ---- |
| η | Efficiency | ---- |

| Symbols | Descriptions | Units |
|---|---|---|
| a | constant | ---- |
| A | Area | $m^2$ |
| AR | Aspect Ratio | ---- |
| b | constant | ---- |
| c | Chord | m |
| $C_D$ | Drag Coefficient | ---- |
| $C_L$ | Lift Coefficient | ---- |
| $C_p$ | Specific Heat at Constant Pressure | J/kg.K |
| D | Diameter | m |
| h | Enthalpy | kJ/kg |
| i | Incidence Angle | degree |
| L | Length (height) | m |
| M | Mach No. | ---- |
| $\dot{m}$ | Mass flow rate | kg/s |
| n | No. of Blade | ---- |
| P | Pressure | Pascal |
| U | Blade Velocity | m/s |
| r | Radius | m |
| R | Gas Constant | kJ/kg.K |
| $R_c$ | Degree of reaction | ---- |
| s | Space | m |
| T | Temperature | K |
| V, w | Fluid Velocity, Relative Velocity | m/s |
| **The compressor inlet temperature ($T_{o1}$)** | | 294K |

**Table 1: The Main Input Data (Al-D**

| | |
|---|---|
| **The compressor inlet pressure ($P_{o1}$)** | 101325 Pa |
| **The compressor inlet velocity ($V_1$)** | 146 m/s |
| **The mean axial velocity ($V_X$)** | 122 m/s |
| **The compressor pressure ratio ($P_{o3}/P_{o1}$)** | 1.23 |
| **The overall compressor pressure ratio** | 4 |
| **The mass flow rate ($\dot{m}$)** | 18.144 kg/s |
| **The rotor blade velocity (U)** | 244 m/s |
| **The angular velocity** | 11500 r.p.m |
| **The blade aspect ratio (AR)** | 3 |
| **The solidity ($\sigma$)** | 1 |
| **The air inlet angle ($\alpha_1$)** | 33° |

**Design Calculations:**

**Table 2: Stage Geometry**

| | $D_r$ (m) | $D_m$ (m) | $D_t$ (m) | L (m) |
|---|---|---|---|---|
| **Rotor inlet** | .3064730 | .4052223 | .5018698 | 9.728426 E-02 |
| **Rotor exit** | .3138668 | .4052223 | .5003454 | 9.023113 E-02 |
| **Stage exit** | .3207271 | .4052223 | .4910624 | 8.501962 E-02 |
| **Comp. exit** | .3605752 | .4052223 | .4502072 | 4.264601 E-02 |

**Table 3: Blade Dimension**

| | Blades No. | Chord Length (m) | Space (m) | AR |
|---|---|---|---|---|
| **Rotor** | 39 | 3.242809E-02 | 3.637267E-02 | 2.93 |
| **Stator** | 34 | 4.722581E-02 | 4.106592E-02 | 2.25 |

**Table 4: Stage Data**

| | | |
|---|---|---|
| **Stage Exit** | 125411.8 (Pa) | 314.9377(K) |
| **Stage Efficiency %** | 88 | ------ |
| **$\Delta$To/To1 for stage** | .069875 | ------ |
| **Compressor Efficiency %** | 84 | |
| **Compressor Exit** | 357452.5(Pa) | 460 (K) |
| **The Power Required** | 3083.518 (kW) | |

**Table 5: Thermodynamics Properties along the Blade**

| D (m) | $P_2$ (Pa) | $T_2$(K) | $\rho_2$ (kg/m$^3$) |
|---|---|---|---|
| .305738 | 103930.24 | 296.576 | 1.22533 |
| .3255473 | 1074035 | 299.6945 | 1.240205 |
| .3505473 | 108585.5 | 300.5109 | 1.255302 |
| .3755473 | 110460 | 303.0857 | 1.269312 |
| **.405223** | **111877.7** | **303.4635** | **1.289135** |
| .4255473 | 113897.6 | 304.6796 | 1.291372 |
| .4505473 | 115272 | 305.7607 | 1.307121 |
| .4755473 | 115622.7 | 307.7281 | 1.310012 |
| .5005473 | 116281.7 | 307.5991 | 1.332690 |

**Table 6: Lift Coefficient along the Blade**

| D (m) | $C_L$ |
|---|---|
| .305738 | .5902831 |
| .3255473 | .5810574 |
| .3505473 | .5707791 |
| .3755473 | .5391446 |
| **.405223** | **.505476** |
| .4255473 | .4580317 |
| .4505473 | .3832497 |
| .4755473 | .2800809 |
| .5005473 | .2030155 |

**Table 7: Blade Angles**

| D (m) | $\alpha^o_1$ | $\alpha^o_2$ | $\beta^o_1$ | $\beta^o_2$ | $\theta^o_{rotor}$ | $\theta^o_{stator}$ | $M_{1rel}$ |
|---|---|---|---|---|---|---|---|
| .30 | 24.27 | 47.13 | 39.12 | 1.33 | 38.82 | -22.77 | .55 |
| .33 | 26.24 | 48.19 | 42.16 | 8.68 | 35.56 | -21.85 | .56 |
| .35 | 28.11 | 49.35 | 46.22 | 15.99 | 31.90 | -21.15 | .57 |
| .38 | 29.90 | 50.65 | 51.20 | 23.45 | 27.09 | -20.66 | .58 |
| **.40** | **33.0** | **53.65** | **53.5** | **32.30** | **20.96** | **-20.35** | **.59** |
| .43 | 35 | 55.4 | 56.77 | 41.64 | 15.85 | -20.30 | .61 |
| .45 | 36.71 | 57.39 | 59.36 | 48.22 | 11.91 | -20.58 | .65 |
| .48 | 38.41 | 59.55 | 61.81 | 54.40 | 7.43 | -21.09 | .68 |
| .50 | 40.43 | 63.61 | 64.45 | 60.57 | 3.31 | -21.88 | .70 |

| D (m) | $\sigma_{rotor}$ | $\sigma_{stator}$ | % $R_n$ |
|---|---|---|---|
| .30 | 1.31 | 1.56 | 17.68 |
| .33 | 1.23 | 1.45 | 27.26 |
| .35 | 1.15 | 1.36 | 35.87 |
| .38 | 1.05 | 1.28 | 44.00 |
| **.40** | **.99** | **1.01** | **50.05** |
| .43 | .94 | 1.03 | 56.02 |
| .45 | .89 | .98 | 60.47 |
| .48 | .85 | .93 | 64.93 |
| .50 | .81 | .9 | 68.72 |

**Table 8: Solidity and Degree of Reaction along Blade**

**At: $\lambda = 40°$ , $\beta_i = 50°$**

**Table 9: Cascade Aerodynamic Forces**

| $C_{L\ cascade}$ | $C_{D\ cascade}$ | $C_{D\ total}$ | Lift (N) | Drag (N) |
|---|---|---|---|---|
| 1.32 | 0.049 | 0.0546 | 568 | 21 |

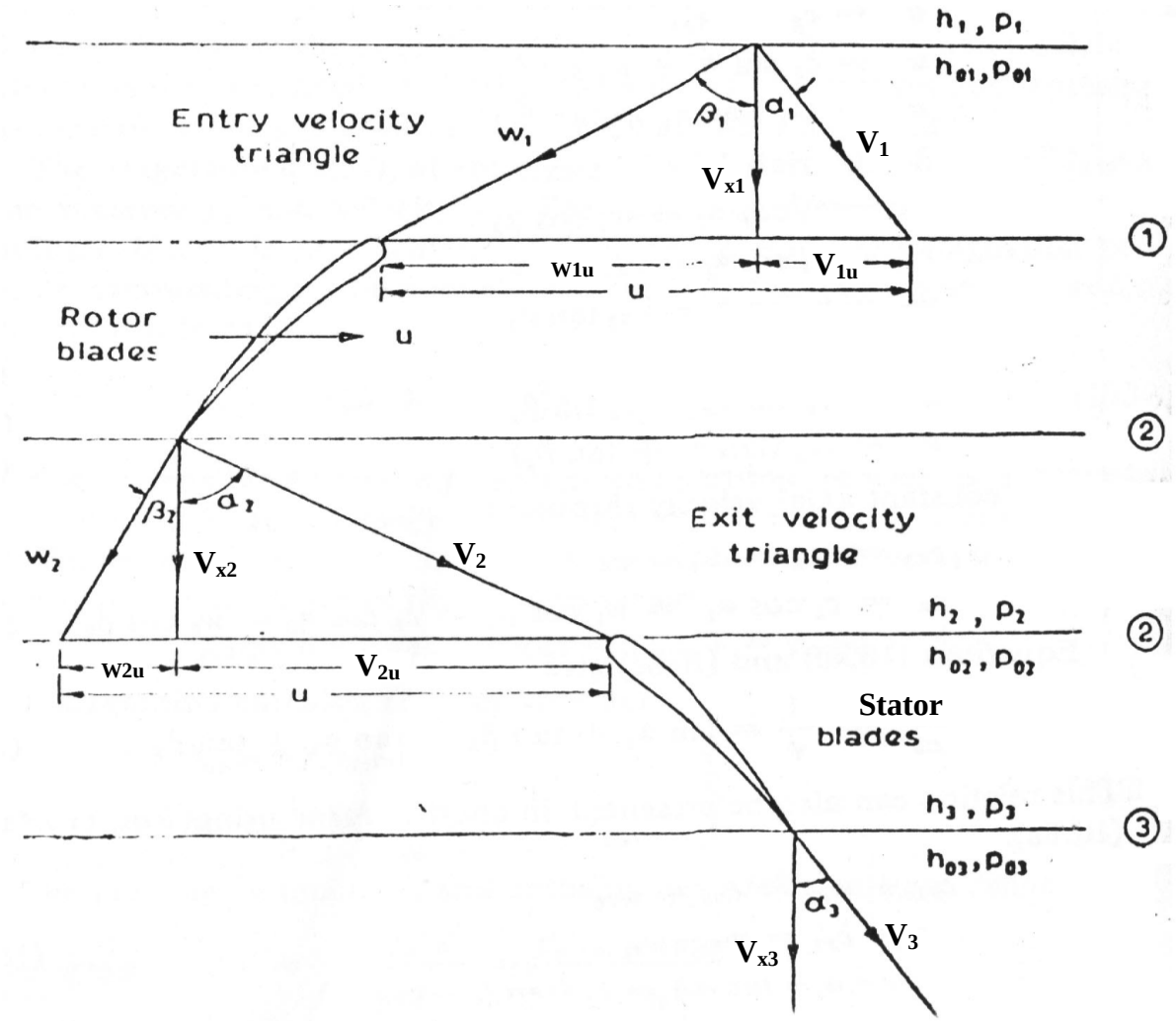


**Fig. 1: Velocity Triangle for Compressor Stage [ Yahya 1983]**

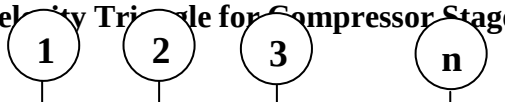

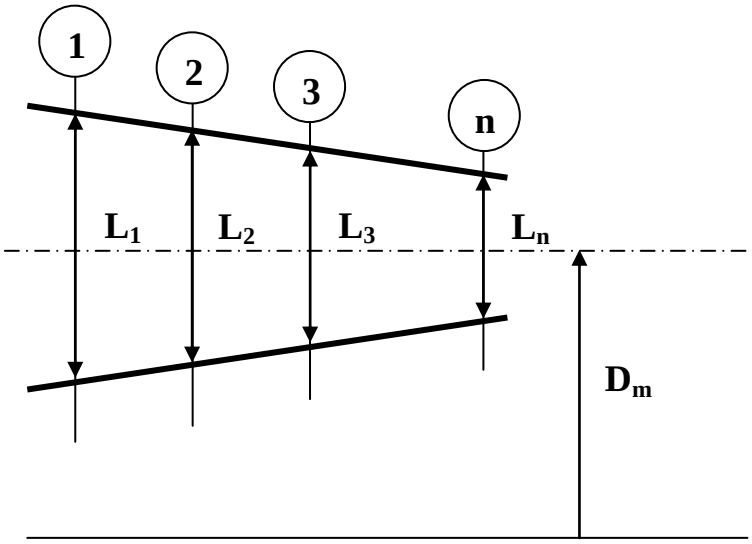


**(a)**

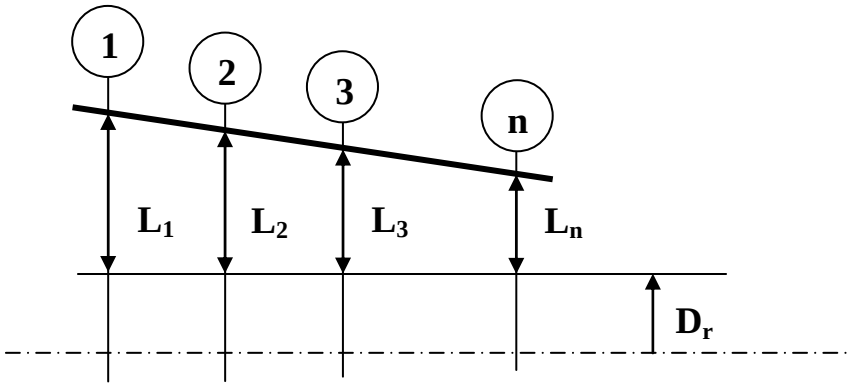


**(b)**

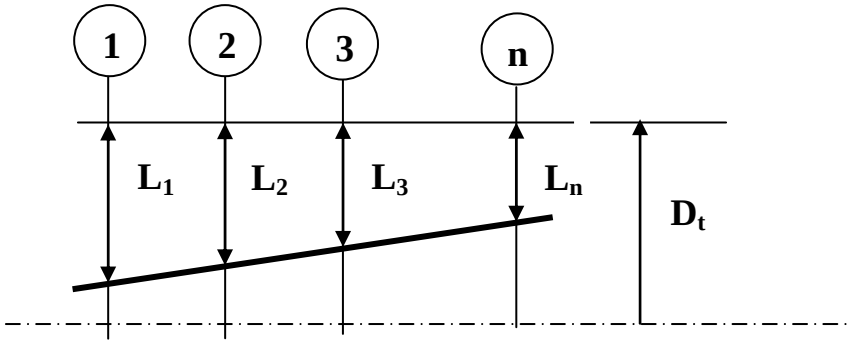


**(c)**

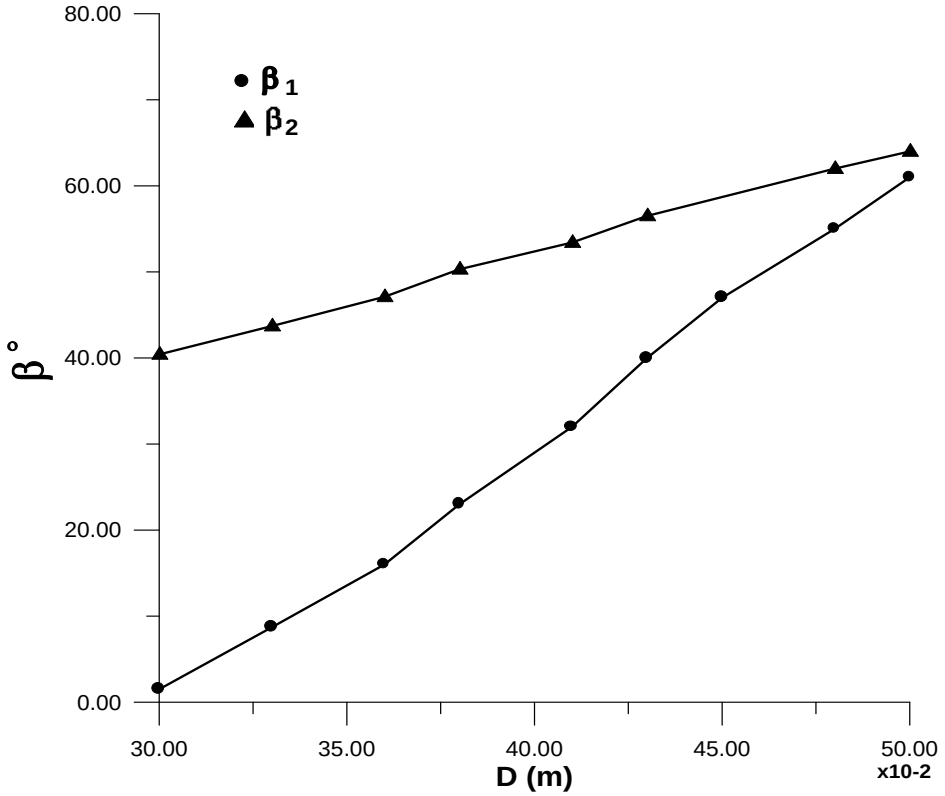


**Fig. 3: Twist of Rotor Angles along Blade Length**

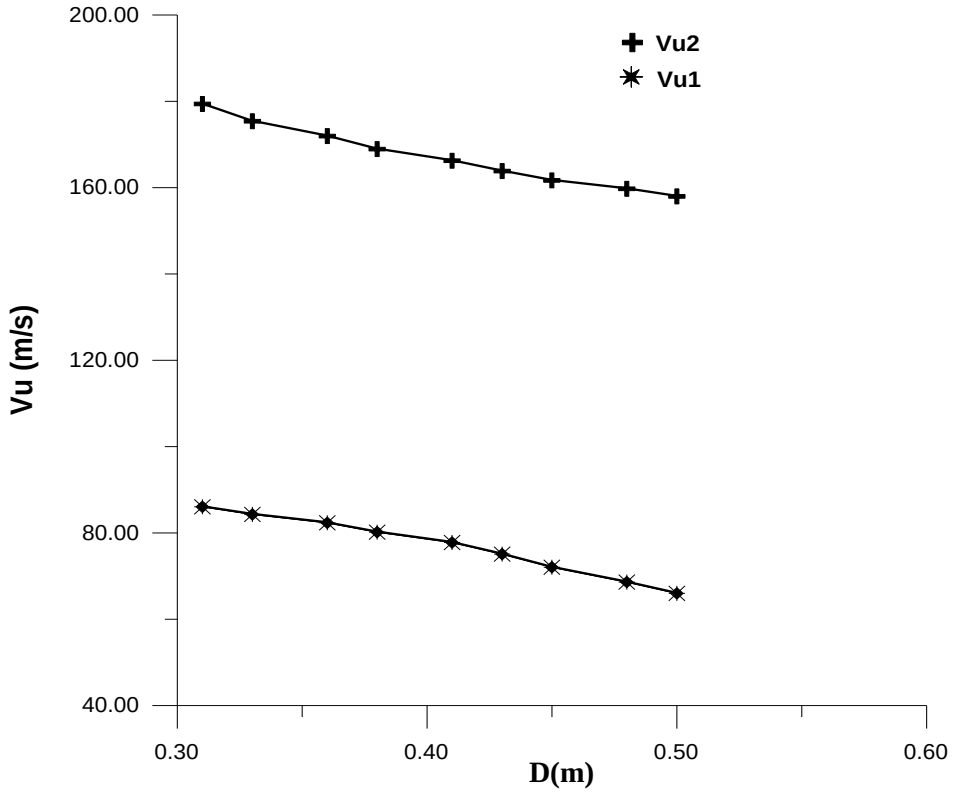


**Fig. 4: Variation of Swirl Velocity along Blade Length**

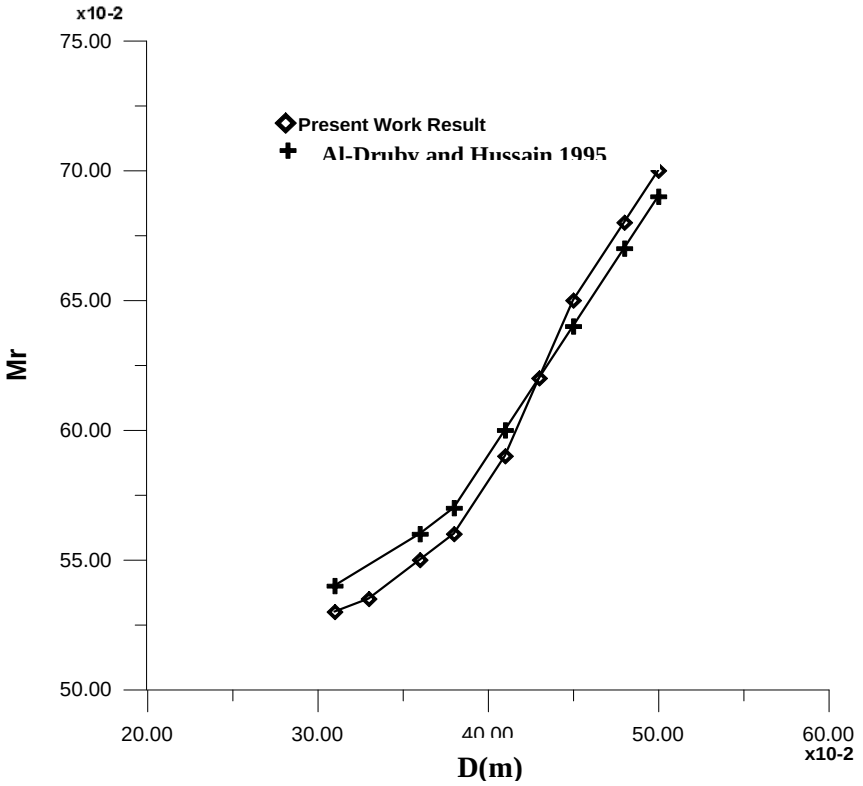


**Fig. 5: Mach No. along Blade Length**

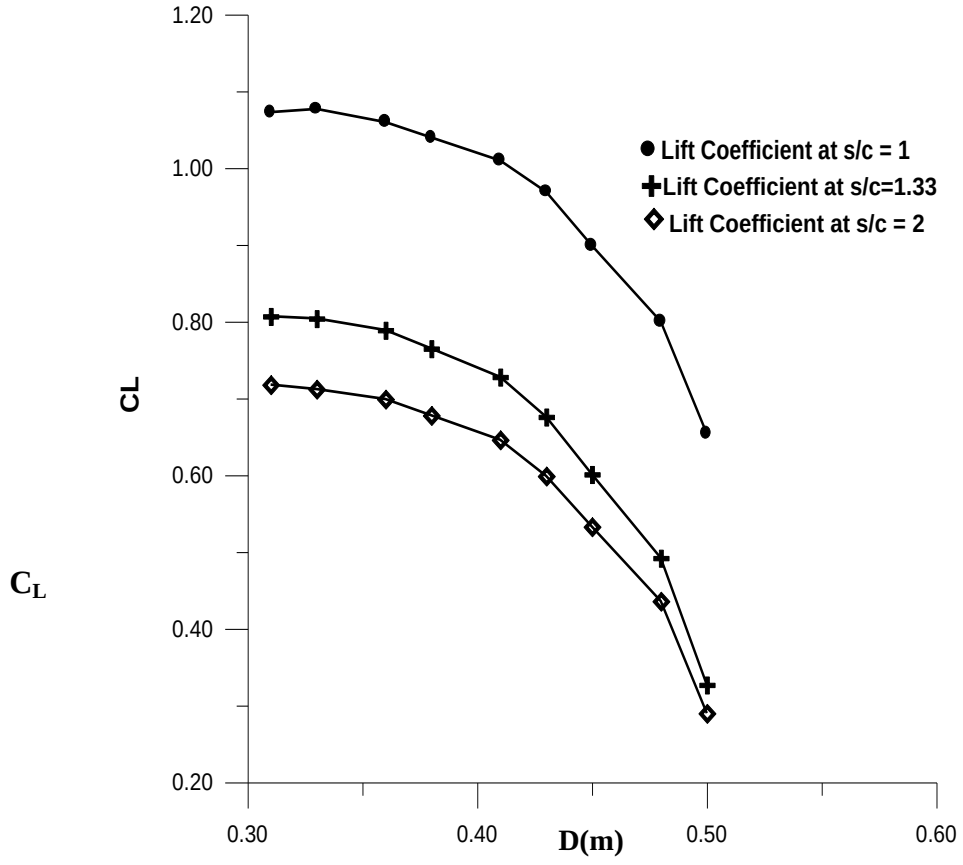


$C_L$

**Fig. 6: Lift Coefficient along Blade Length at Different Solidities**

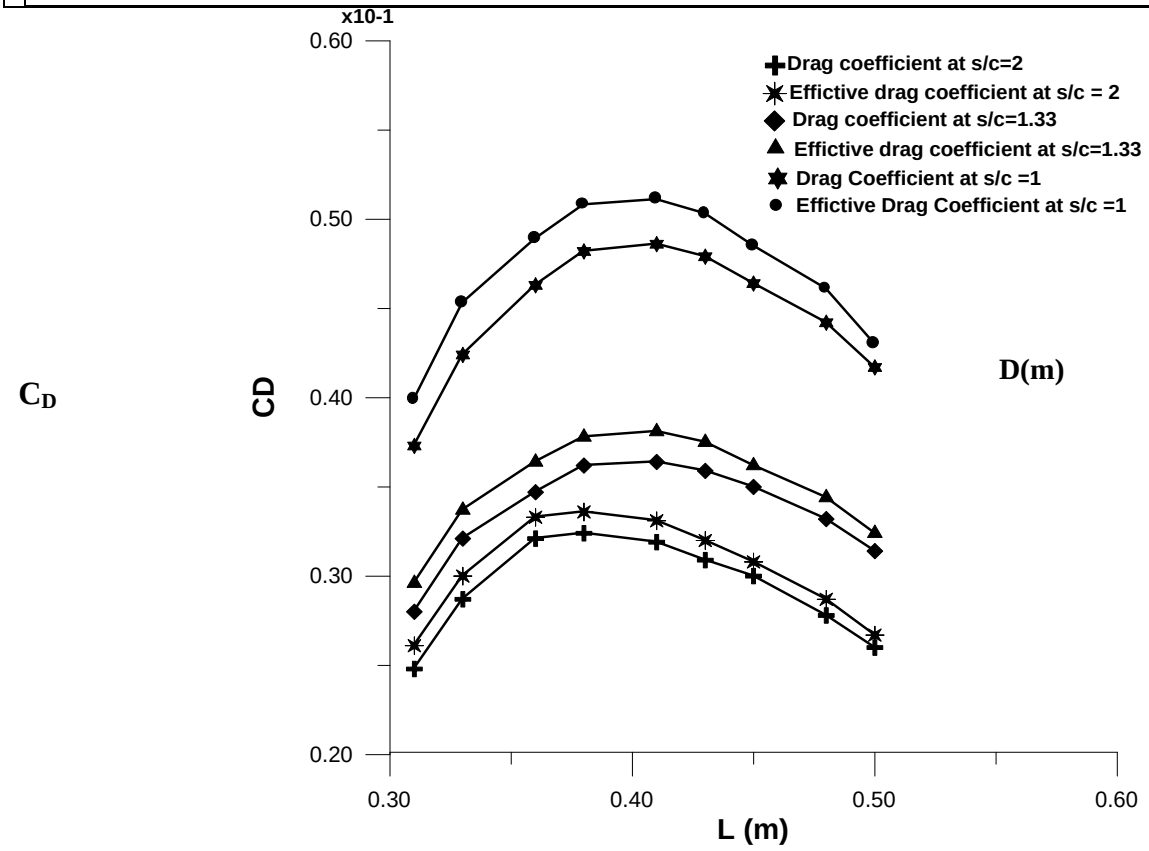


$C_D$

**Fig. 7: Drag Coefficient along Blade Length at Different Solidities**

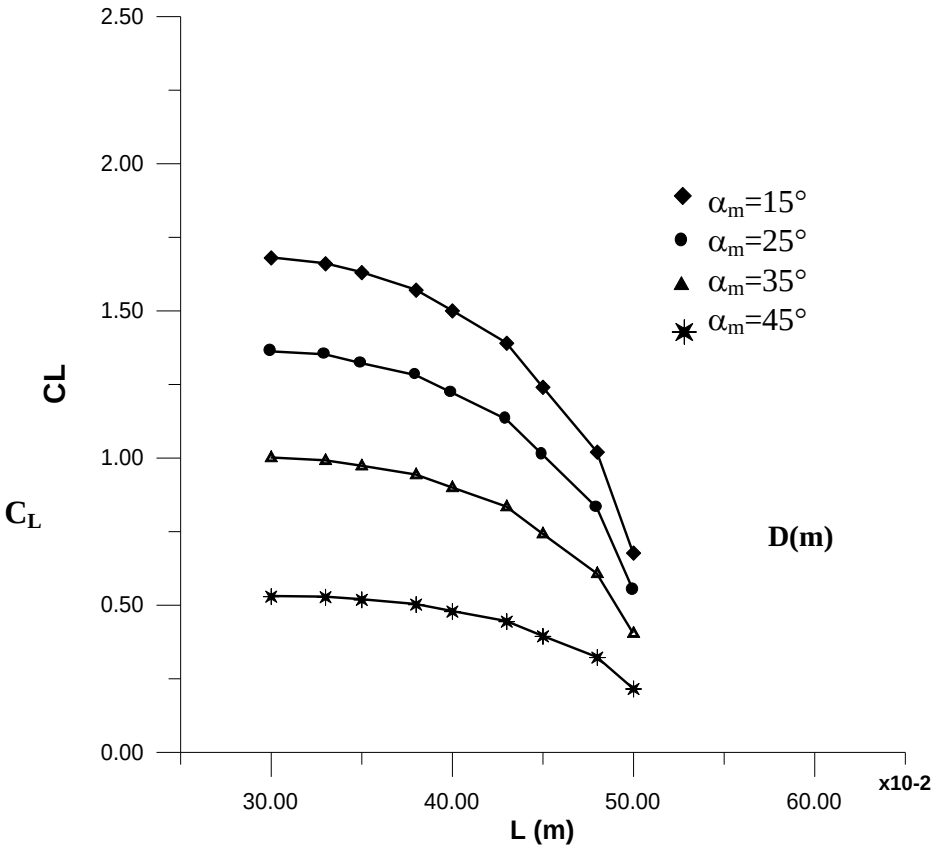


$C_L$

**Fig. 8: Lift Coefficient along Blade Length at Different Mean Flow Angle**

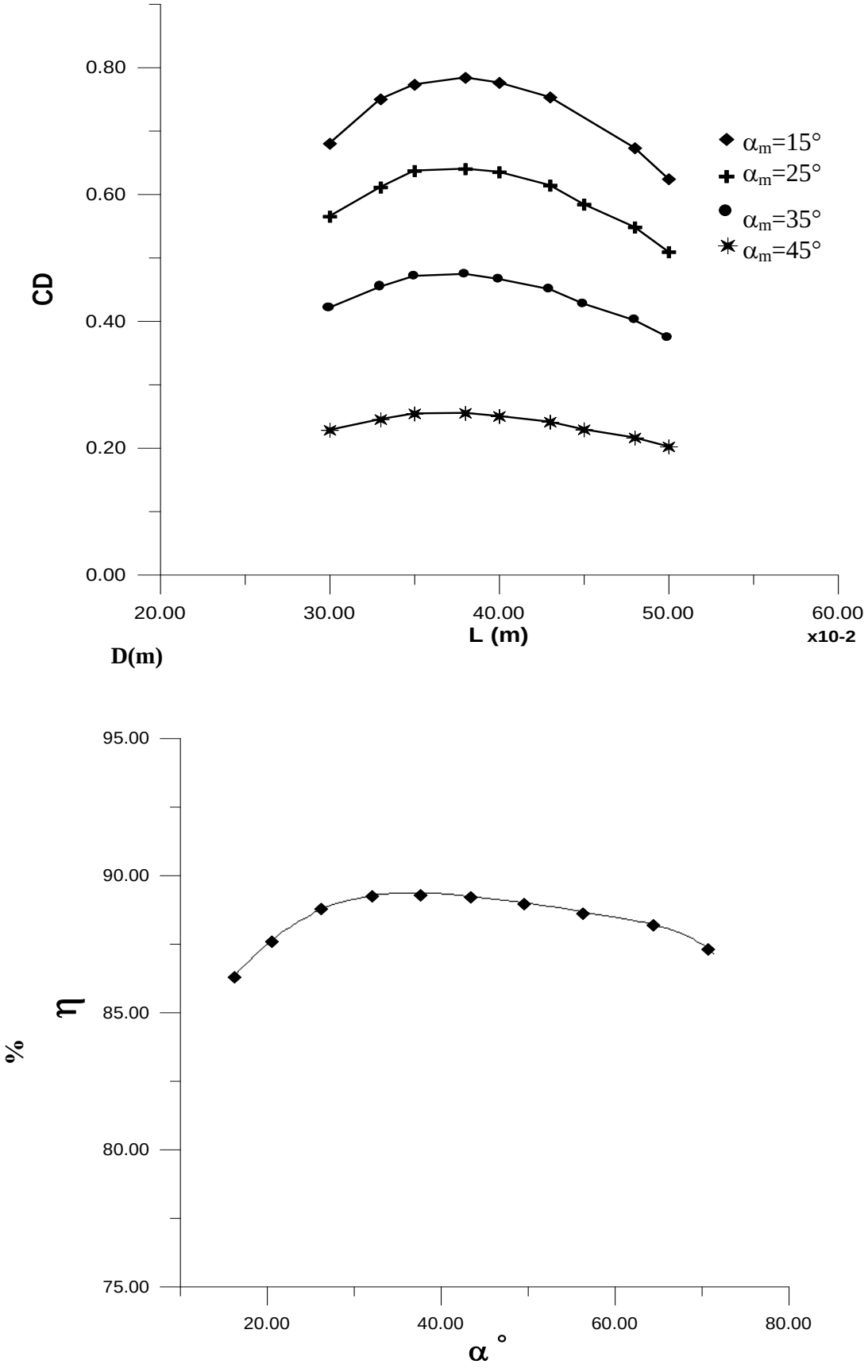


**Fig. 10: Cascade Efficiency versus Mean Flow Angle**